Difference Frequency Generation Spectroscopy as a Vibrational Optical Activity Measurement Tool

Sangheon Cheon[†] **and Minhaeng Cho***[,†,‡]

Department of Chemistry and Center for Multidimensional Spectroscopy, Korea University, Seoul 136-701, Korea, and Multidimensional Spectroscopy Laboratory, Korea Basic Science Institute, Seoul 136-713, Korea

Received: October 31, 2008; Revised Manuscript Received: December 17, 2008

Vibrational optical activity (VOA) of chiral molecules in condensed phases can be studied by using vibrational circular dichroism and Raman optical activity measurement techniques. Recently, IR-vis sum frequency generation has shown to be an alternative VOA measurement method. Such a three-wave-mixing method employing a polarization modulation technique can be a potentially useful VOA measurement tool. Here, a theoretical description of difference frequency generation (DFG) employing circularly polarized visible radiations is presented. Frequency scanning to obtain a VOA-DFG spectrum is achieved by controlling the difference between the two electronically nonresonant incident radiation frequencies. If the two incident beams are linearly polarized and their polarization directions are perpendicular to each other, one can selectively measure the all-electric-dipole-allowed chiral component of the DFG susceptibility. In addition, by using circularly polarized beams and taking the DFG difference intensity signal, which is defined as the difference between left and right circularly polarized DFG signals, additional chiral susceptibility components originating from the electric quadrupole transition can be measured. The DFG as a novel VOA measurement technique for solution samples containing chiral molecules will therefore be a useful coherent spectroscopic tool for determining absolute configuration of chiral molecules in condensed phases.

I. Introduction

A better understanding of optical activity properties is very important for studies of the molecular basis of various biological activities, because most natural products and biomolecules such as proteins and nucleic acids exhibit a variety of interesting optical activities.[1] The optical activity is, by definition, related to a differential interaction of a chiral molecule with left and right circularly polarized (LCP and RCP) radiations.[2] Although IR absorption spectroscopy has served as an excellent and useful tool for studying structure and dynamics of complex molecules,[3] the IR analogue of circular dichroism, which is called vibrational circular dichroism (VCD), is sensitive to absolute configuration of chiral molecules in condensed phases and has been found to be better in frequency resolution than IR absorption spectroscopy.[4−9] Note that the VCD measures the differential absorbance of LCP and RCP IR radiation by a chiral molecule so that the VCD peak can have either positive or negative sign depending on the angle between the transition electric and magnetic dipoles of a given vibrational excitation. This additional sign information is crucial for the structure determination of a chiral molecule.

A Raman version of vibrational optical activity spectroscopy is the Raman optical activity (ROA), which has been extensively used since its discovery by Barron and co-workers.[10−14] Here, the ROA is usually determined by measuring the circular intensity difference ΔI ($= I(R) - I(L)$, where $I(R)$ and $I(L)$ are the Raman scattering field intensities when the incident radiation is right and left circularly polarized, respectively).[14,15] ROA technique has become a powerful chiro-optical measurement tool, which is applicable to a wide range of chiral samples, from small organic molecules to intact viruses. These two different methods, VCD and ROA, can provide complementary information on the vibrational optical activity of a chiral molecule.

In addition to these VOA measurement techniques, it was experimentally demonstrated that the IR-visible sum frequency generation (IV-SFG) technique can be an alternative VOA measurement tool.[16−21] Although IV-SFG spectroscopy has been extensively used to study vibrational dynamics of adsorbed molecules on surfaces or at interfaces,[22−33] it can also be applied to chiral molecules in solutions to measure the corresponding vibrational optical activity susceptibility. An early experiment was performed by using linearly polarized IR and visible radiations to generate the IV-SFG signal field.[16] To successfully carry out the IV-SFG measurements for chiral molecules in an isotropic medium, the polarization directions of the two incident radiations and the IV-SFG electric field vector had to be properly controlled so that they were mutually perpendicular to one another. Then, the chiral component of the susceptibility was found to be measurably large when the antisymmetric Raman tensor elements of a chiral molecule did not vanish. Later, we theoretically showed that there exist different types of VOA SFG techniques utilizing circularly polarized radiations.[34−37] The circular intensity difference, which is defined as the difference between the IV-SFG signal with an LCP radiation and that with an RCP radiation, was found to be chirality-sensitive.

In this article, we shall present a quantum electrodynamics theory on the difference frequency generation, which is believed to be an alternative and potentially useful vibrational optical activity measurement technique for chiral molecules in solutions. If the difference frequency is close to one of the vibrational frequencies of a chiral molecule in an isotropic medium, the vibrationally resonant-enhanced DFG signal can be detected.

* To whom correspondence should be addressed. E-mail: mcho@korea.ac.kr.
[†] Korea University.
[‡] Korea Basic Science Institute.

10.1021/jp809652x CCC: $40.75 © 2009 American Chemical Society
Published on Web 02/19/2009

If the two incident visible radiations, which are electronically nonresonant, are linearly polarized and if an appropriate detection scheme is used, as will be shown in this article, one can measure a particular vibrational optical activity (see the first energy level diagram in Figure 1). The other types of VOA-DFG processes shown in Figure 1 will also be theoretically discussed in detail in sections IV−VI. The main result will be summarized in section VII.

II. Model Hamiltonian and DFG Transition Amplitude

From the multipolar expansion form of the radiation−matter interaction Hamiltonian in the quantum electrodynamics theory,[38,39] we have

$$H_{\mathrm{int}} = -\varepsilon_0^{-1}\int \mu_i \delta(\mathbf{r}-\mathbf{R}) d_i^{\perp}(\mathbf{r})\,\mathrm{d}V - \int m_i \delta(\mathbf{r}-\mathbf{R}) b_i(\mathbf{r})\,\mathrm{d}V - \varepsilon_0^{-1}\int Q_{ij}\delta(\mathbf{r}-\mathbf{R})\nabla_j d_i^{\perp}(\mathbf{r})\,\mathrm{d}V \quad (1)$$

where μ_i, m_i, and Q_{ij} are the electric dipole, magnetic dipole, and electric quadrupole operators, respectively. Note that only those terms that are zero and first order with respect to $\mathbf{k}$ are taken into consideration in eq 1 and that the Einstein summation convention is used. ε_0 is the vacuum permittivity. The position vector of the molecular center is $\mathbf{R}$. V is the quantization volume. The first term in eq 1 is just the electric dipole−electric field interaction. The second term describes magnetic dipole−magnetic field interaction. Finally, the third term represents the interaction between the electric quadrupole and electric field gradient. Typically, the last two terms are much smaller than the first one by 2 to 3 orders of magnitude, and thus they were ignored in the conventional light absorption and scattering spectroscopy. However, they play an important role in determining optical activity of a chiral molecule.[39]

The mode-expanded transverse electric and magnetic fields are, respectively,

$$\mathbf{d}^{\perp}(\mathbf{r}) = i\sum_{k,\lambda}\left(\frac{\hbar c k \varepsilon_0}{2V}\right)^{1/2}\{\mathbf{e}^{(\lambda)}(\mathbf{k})a^{(\lambda)}(\mathbf{k})e^{i\mathbf{k}\cdot\mathbf{r}} - \bar{\mathbf{e}}^{(\lambda)}(\mathbf{k})a^{+(\lambda)}(\mathbf{k})e^{-i\mathbf{k}\cdot\mathbf{r}}\}$$

$$\mathbf{b}(\mathbf{r}) = i\sum_{k,\lambda}\left(\frac{\hbar k}{2\varepsilon_0 c V}\right)^{1/2}\{\mathbf{b}^{(\lambda)}(\mathbf{k})a^{(\lambda)}(\mathbf{k})e^{i\mathbf{k}\cdot\mathbf{r}} - \bar{\mathbf{b}}^{(\lambda)}(\mathbf{k})a^{+(\lambda)}(\mathbf{k})e^{-i\mathbf{k}\cdot\mathbf{r}}\} \quad (2)$$

where the wavevector of the electromagnetic field is denoted as $\mathbf{k}$. c is the speed of light. The unit vector of the electric and magnetic field vectors of the $(\mathbf{k},\lambda)$ mode are $\mathbf{e}^{(\lambda)}(\mathbf{k})$ and $\mathbf{b}^{(\lambda)}(\mathbf{k})$, respectively, and they are related to each other as $\mathbf{b}^{(\lambda)}(\mathbf{k}) = \hat{\mathbf{k}} \times \mathbf{e}^{(\lambda)}(\mathbf{k})$, where $\hat{\mathbf{k}} = \mathbf{k}/|\mathbf{k}|$. The creation and annihilation operators of the $(\mathbf{k},\lambda)$ mode are $a^{+(\lambda)}(\mathbf{k})$ and $a^{(\lambda)}(\mathbf{k})$, respectively. The bar in $\bar{\mathbf{e}}^{(\lambda)}(\mathbf{k})$ or $\bar{\mathbf{b}}^{(\lambda)}(\mathbf{k})$ means complex conjugate.

Difference frequency generation, as a three-wave-mixing process, involves interactions with two incident fields and an interaction with a vacuum field.[40] In this article, it will be assumed that the two incident visible fields are nonresonant to electronic transitions of chiro-optical chromophores dissolved in condensed phases. Denoting the two wavevectors as $\mathbf{k_1}$ and $\mathbf{k_2}$, we give the wavevector of the radiated DFG field, denoted as $\mathbf{k_3}$, as $\mathbf{k_3} = \mathbf{k_1} - \mathbf{k_2}$, because of the phase-matching condition. Although an incoherent DFG process where signal intensity is proportional to the number n of chromophores is also allowed, it is negligibly small in comparison to that of the coherent DFG signal, which is proportional to the square of n. Thus, the incoherent DFG process will not be considered in this article.

A. Transition Amplitude. To calculate the coherent DFG signal intensity, which is related to the DFG transition probability, one should first consider corresponding third-order optical transition amplitude. The initial and final states associated with the DFG are

$$|i\rangle = |E_0;\, n_1(\mathbf{k_1},\lambda_1),\, n_2(\mathbf{k_2},\lambda_2)\rangle$$
$$|f\rangle = |E_0;\, (n_1-1)(\mathbf{k_1},\lambda_1),\, (n_2+1)(\mathbf{k_2},\lambda_2),\, 1(\mathbf{k_3},\lambda_3)\rangle \quad (3)$$

where n_1 and n_2 are the occupation numbers of the two incident visible fields. A single photon state of the DFG signal field is denoted as $1(\mathbf{k_3},\lambda_3)$. Overall, one photon of the $\mathbf{k_1}$ field is split into two photons with $\mathbf{k_2}$ and $\mathbf{k_3}$ momenta, but the system state with energy E_0 remains the same.

Treating the approximate radiation−matter interaction Hamiltonian in eq 1, which is valid up to the first order in $\mathbf{k}$, as a perturbation, one can find a number of optical transition pathways contributing to the DFG transition M_{DFG} from $|i\rangle$ to $|f\rangle$. Since the electric quadrupole−electric field and magnetic dipole−magnetic field interactions are 2 to 3 orders of magnitude smaller than the electric dipole−electric field interaction,[38] one can expand M_{DFG} with respect to m and Q as

$$M_{\mathrm{DFG}} = M_{\mathrm{DFG}}^{(0)} + M_{\mathrm{DFG}}^{(1)}(m) + M_{\mathrm{DFG}}^{(1)}(Q) + \ldots \quad (4)$$

Here, the zero-order term $M_{\mathrm{DFG}}^{(0)}$ is an all-electric-dipole contribution, whereas the second and third terms are linearly proportional to magnetic dipole and electric quadrupole, respectively. In eq 4, we shall ignore the second- and third-order terms with respect to m and/or Q. Even with this truncation approximation, there are 42 different transition pathways contributing to the DFG. Among them, only those that are vibrationally resonant-enhanced terms will be considered. That is to say, those terms with $\omega_1 - \omega_2 \cong \omega_v$, where ω_1 and ω_2 are the two incident field frequencies and ω_v is one of the vibrational frequencies, are included. Since the incident visible radiations are nonresonant to electronic transitions of the molecular systems of interest, we shall use the Placzek approximation. Then, we find that the transition amplitude associated with the DFG, which is again valid up to the first order in $\mathbf{k}$, is given as

$$\begin{aligned} M_{\mathrm{DFG}} \cong i\left(\frac{\hbar c}{2\varepsilon_0 V}\right)^{3/2}\{n_1(n_2+1)k_1k_2k_3\}^{1/2}\times \\ \Big[\bar{e}_i^{(\lambda_3)}(\mathbf{k}_3)\bar{e}_j^{(\lambda_2)}(\mathbf{k}_2)e_k^{(\lambda_1)}(\mathbf{k}_1)\langle\beta_{ijk}^{\mu\alpha}\rangle + \\ \frac{1}{c}\bar{e}_i^{(\lambda_3)}(\mathbf{k}_3)\bar{e}_j^{(\lambda_2)}(\mathbf{k}_2)b_k^{(\lambda_1)}(\mathbf{k}_1)\langle\beta_{ijk}^{\mu G}\rangle + \\ \frac{1}{c}\bar{e}_i^{(\lambda_3)}(\mathbf{k}_3)\bar{b}_j^{(\lambda_2)}(\mathbf{k}_2)e_k^{(\lambda_1)}(\mathbf{k}_1)\langle\beta_{ijk}^{\mu\bar{G}}\rangle + \\ \frac{1}{c}\bar{b}_i^{(\lambda_3)}(\mathbf{k}_3)\bar{e}_j^{(\lambda_2)}(\mathbf{k}_2)e_k^{(\lambda_1)}(\mathbf{k}_1)\langle\beta_{ijk}^{m\alpha}\rangle + \\ i\bar{e}_i^{(\lambda_3)}(\mathbf{k}_3)\bar{e}_j^{(\lambda_2)}(\mathbf{k}_2)e_k^{(\lambda_1)}(\mathbf{k}_1)k_l\langle\beta_{ijkl}^{\mu A}\rangle - \\ i\bar{e}_i^{(\lambda_3)}(\mathbf{k}_3)\bar{e}_j^{(\lambda_2)}(\mathbf{k}_2)e_k^{(\lambda_1)}(\mathbf{k}_1)k_m'\langle\beta_{ijkm}^{\mu\bar{A}}\rangle - \\ i\bar{e}_i^{(\lambda_3)}(\mathbf{k}_3)\bar{e}_j^{(\lambda_2)}(\mathbf{k}_2)e_k^{(\lambda_1)}(\mathbf{k}_1)k_n''\langle\beta_{injk}^{Q\alpha}\rangle\Big] \end{aligned} \quad (5)$$

Here, the seven molecular hyperpolarizability tensors in eq 5 are defined as

$$\beta_{ijk}^{\mu\alpha} = \sum_{s} \frac{\mu_i^{0s}\alpha_{jk}^{s0}}{E_{s0} - \hbar\omega_3 + i\Gamma_s}$$

$$\beta_{ijk}^{\mu G} = \sum_{s} \frac{\mu_i^{0s}G_{jk}^{s0}}{E_{s0} - \hbar\omega_3 + i\Gamma_s}$$

$$\beta_{ijk}^{\mu \bar{G}} = \sum_{s} \frac{\mu_i^{0s}\bar{G}_{jk}^{s0}}{E_{s0} - \hbar\omega_3 + i\Gamma_s}$$

$$\beta_{ijk}^{m\alpha} = \sum_{s} \frac{m_i^{0s}\alpha_{jk}^{s0}}{E_{s0} - \hbar\omega_3 + i\Gamma_s}$$

$$\beta_{ijkl}^{\mu A} = \sum_{s} \frac{\mu_i^{0s}A_{jkl}^{s0}}{E_{s0} - \hbar\omega_3 + i\Gamma_s}$$

$$\beta_{ijkm}^{\mu \bar{A}} = \sum_{s} \frac{\mu_i^{0s}\bar{A}_{jkm}^{s0}}{E_{s0} - \hbar\omega_3 + i\Gamma_s}$$

$$\beta_{injk}^{Q\alpha} = \sum_{s} \frac{Q_{in}^{0s}\alpha_{jk}^{s0}}{E_{s0} - \hbar\omega_3 + i\Gamma_s} \quad (6)$$

where Γ_s is the vibrational dephasing constant and the vibrational ground, and first excited states are denoted as 0 and s, respectively. μ_i^{0s} and m_i^{0s} are the ith vector element of the transition electric dipole and transition magnetic dipole matrix elements. In eq 5, k_l, k_l', and k_l'' are the lth vector element of $\mathbf{k_1}$, $\mathbf{k_2}$, and $\mathbf{k_3}$, respectively. The $[i,n]$th tensor element of the transition electric quadrupole matrix element is denoted as Q_{in}^{0s}. The elements of the polarizability, magnetic dipole-ROA tensors, $G_{ij}^{\phi\psi}(\omega)$ and $\bar{G}_{ij}^{\phi\psi}(\omega)$, and electric quadrupole-ROA tensors, $A_{ijl}^{\phi\psi}(\omega)$ and $\bar{A}_{ijl}^{\phi\psi}(\omega)$, are given as[14,41]

$$\alpha_{ij}^{\phi\psi}(\omega) = \sum_{r}\left(\frac{\mu_i^{\phi r}\mu_j^{r\psi}}{E_{r0} - \hbar\omega} + \frac{\mu_j^{\phi r}\mu_i^{r\psi}}{E_{r0} + \hbar\omega}\right)$$

$$G_{ij}^{\phi\psi}(\omega) = \sum_{r}\left(\frac{\mu_i^{\phi r}m_j^{r\psi}}{E_{r0} - \hbar\omega} + \frac{m_j^{\phi r}\mu_i^{r\psi}}{E_{r0} + \hbar\omega}\right)$$

$$\bar{G}_{ij}^{\phi\psi}(\omega) = \sum_{r}\left(\frac{m_i^{\phi r}\mu_j^{r\psi}}{E_{r0} - \hbar\omega} + \frac{\mu_j^{\phi r}m_i^{r\psi}}{E_{r0} + \hbar\omega}\right)$$

$$A_{ijl}^{\phi\psi}(\omega) = \sum_{r}\left(\frac{\mu_i^{\phi r}Q_{jl}^{r\psi}}{E_{r0} - \hbar\omega} + \frac{Q_{jl}^{\phi r}\mu_i^{r\psi}}{E_{r0} + \hbar\omega}\right)$$

$$\bar{A}_{ijl}^{\phi\psi}(\omega) = \sum_{r}\left(\frac{Q_{il}^{\phi r}\mu_j^{r\psi}}{E_{r0} - \hbar\omega} + \frac{\mu_j^{\phi r}Q_{il}^{r\psi}}{E_{r0} + \hbar\omega}\right) \quad (7)$$

Here, the summation is over all vibronic states except for the ground state.

In Figure 2, the respective Feynman diagrams that are associated with the seven terms in eq 5 are depicted. The first term in eq 5, which corresponds to diagram (1) in Figure 2, is all-electric-dipole contribution to $M_{\mathrm{DFG}}^{(0)}$, since the three radiation−matter interactions are described by the first term in eq 1. Diagrams (2)−(4) involve one magnetic dipole−magnetic field interaction so that they contribute to $M_{\mathrm{DFG}}^{(1)}(m)$. Diagrams (5)−(7) involve one electric quadrupole−electric field interaction and contribute to $M_{\mathrm{DFG}}^{(1)}(Q)$.

Usually, three-wave-mixing spectroscopy such as SFG and DFG has been applied to molecular systems with a broken centrosymmetry, such as adsorbed molecules on surface or at interface. In this case, since molecules are not randomly oriented,

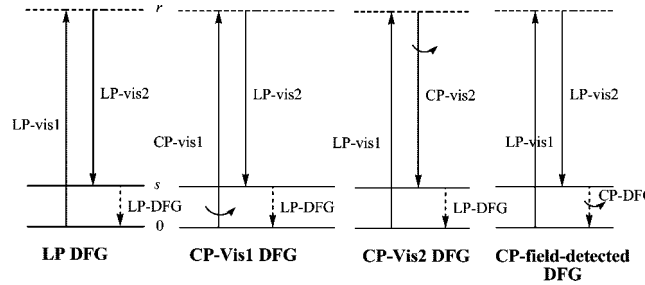

Figure 1. Energy level diagrams of four different DFG processes. The first case is when the incident visible radiations and radiated DFG signal field are linearly polarized. The second (third) case is when the incident visible-1 (visible-2) radiation is circularly polarized. The fourth case is when the circularly polarized components of the DFG field are detected. The molecular quantum states $|0\rangle$ and $|s\rangle$ are vibrational ground and excited states, respectively, and $|r\rangle$ denotes an electronically nonresonant virtual state.

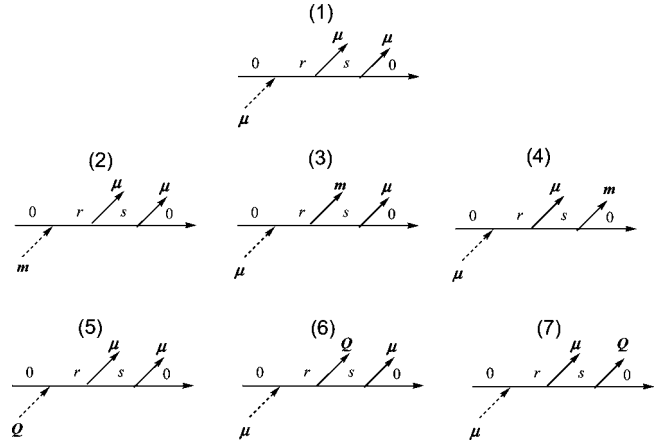

Figure 2. Feynman diagrams associated with seven terms in eq 5. The incoming dashed arrow represents an absorptive interaction, whereas the outgoing solid arrow describes an emission process.

the transition amplitude in eq 5 should be averaged over such an orientation distribution. The orientation-averaged all-electric-dipole term is 2 to 3 orders of magnitude larger than the other correction terms $M_{\mathrm{DFG}}^{(1)}(m)$ and $M_{\mathrm{DFG}}^{(1)}(Q)$:

$$M_{\mathrm{DFG}}^{(0)} \gg M_{\mathrm{DFG}}^{(1)}(m) \approx M_{\mathrm{DFG}}^{(1)}(Q) \quad (8)$$

Consequently, the magnetic dipole and electric quadrupole contributions to the surface SFG and DFG signals were safely ignored in the interpretations of experimentally measured spectra.

However, in the case where chiral molecules are dissolved in an isotropic medium, which is the molecular system of interest in this article, the inequality in eq 8 is not always valid. In a solution sample containing chiral molecules, for example, it is necessary to carry out rotational averages of the third or fourth rank tensorial hyperpolarizabilities in eq 6 over randomly oriented molecules. The angle bracket in eq 5 means that the tensorial quantity inside the bracket should be averaged over all possible orientations. In the following sections, for a few beam configurations with specified polarization states of the incident radiations, we shall present theoretical results for rotational averaged DFG transition amplitudes and signal intensities. Before that, the relationship between the DFG transition amplitude and signal intensity should be discussed first.

B. DFG Intensity. Once the transition amplitude for a given DFG is determined, by using Fermi's golden rule expression, the transition rate can be calculated by

$$\Gamma = \frac{2\pi}{\hbar} N^2 |\langle M_{\mathrm{DFG}} \rangle|^2 \rho_{\mathrm{rad}} \tag{9}$$

where $\rho_{\mathrm{rad}} = [k_3^2 V/(8\pi^3 \hbar c)]\, \mathrm{d}\Omega$ and Ω is the solid angle. Then, the coherent DFG signal intensity is given as $I_{\mathrm{DFG}} = (\mathrm{d}\Gamma/\mathrm{d}\Omega)\hbar c k_3$, so that we have

$$I_{\mathrm{DFG}} = (N^2 k_3{}^3 V/4\pi^2 \hbar) |\langle M_{\mathrm{DFG}} \rangle|^2 \tag{10}$$

Inserting the third-order transition amplitude given in eq 5 into eq 10, one can obtain the general expression for the coherent DFG intensity for an arbitrary experimental beam configuration.

III. Linearly Polarized DFG and Perpendicular Detection Scheme

Among the seven hyperpolarizability contributions in eq 5, one can selectively measure the all-electric-dipole term by using a specifically designed experimental configuration discussed in this section. Let us consider the case where the incident visible-1 and -2 radiations are linearly polarized lights. They cross at the center of the chiral solution sample at an angle θ as shown in Figure 3. Without loss of generality, the propagation direction of the visible-1 radiation is assumed to be parallel to the *Z*-axis in a space-fixed frame and its polarization direction is on the *X*-axis.[35] The propagation direction of the visible-2 radiation is shown in Figure 3. Thus, the two wavevectors and unit vectors of the incident radiations are

$$\begin{aligned} \mathbf{k_1} &= \hat{Z} \\ \mathbf{k_2} &= \hat{X} \sin\theta + \hat{Z} \cos\theta \\ \mathbf{e}^{(1)} &= \hat{X} \\ \mathbf{e}^{(2)} &= \hat{X} \cos\theta - \hat{Z} \sin\theta \end{aligned} \tag{11}$$

Note that the polarization directions of the two incident beams are on the $X-Z$ plane. Placing a linear polarizer in between the sample and a detector, one can selectively measure the *Y*-component of the DFG signal field (i.e., $\mathbf{e}^{(3)} = \hat{Y}$). Since the polarization direction of the detected signal field is perpendicular to those of the incident beams (i.e., $\mathbf{e}^{(1)} \perp \mathbf{e}^{(3)}$ and $\mathbf{e}^{(2)} \perp \mathbf{e}^{(3)}$), we shall refer to this experimental geometry as perpendicular detection scheme.

In this case of linearly polarized (LP) DFG measurement at a fixed incident beam crossing angle θ, one can carry out the rotational average of the third- and fourth-rank tensors given in eq 6 over randomly oriented chiral molecules. It turns out that only the all-electric-dipole term does not vanish in this case, and the DFG transition amplitude is given as

$$\langle M_{\mathrm{DFG}} \rangle = -\frac{iC \sin\theta}{12\sqrt{2}} \varepsilon_{\lambda\mu\nu} \beta^{\mu\alpha}_{\lambda\mu\nu} \tag{12}$$

where $\varepsilon_{\lambda\mu\nu}$ is the antisymmetric Levi−Civita tensor:

$$\varepsilon_{XYZ} = \varepsilon_{YZX} = \varepsilon_{ZXY} = -\varepsilon_{XZY} = -\varepsilon_{YXZ} = -\varepsilon_{ZYX} = 1 \tag{13}$$

and

$$\varepsilon_{\lambda\mu\nu} = 0 \tag{14}$$

otherwise.

The constant *C* in eq 12 is related to the intensities of the incident visible radiations and defined as

$$C \equiv \left(\frac{\hbar c}{\varepsilon_0 V}\right)^{3/2} \{n_1(n_2+1)k_1 k_2 k_3\}^{1/2} \tag{15}$$

In eq 12, the subscripts λ, μ, and ν represent one of the Cartesian coordinate axes in a molecule-fixed frame and $\beta^{\mu\alpha}_{\lambda\mu\nu}$ is the corresponding hyperpolarizability determined in the molecule-fixed frame. Note that the rotational average of any arbitrary third-rank tensor, $\langle \beta_{ijk} \rangle$, is given as $\langle \beta_{ijk} \rangle = \varepsilon_{ijk}\varepsilon_{\lambda\mu\nu}\beta_{\lambda\mu\nu}/6$, where *i*, *j*, and *k* represent one of the axes in a space-fixed frame.[39] From eq 12 with eq 10, we find that the LP DFG signal intensity is

$$I_{\mathrm{LP\text{-}DFG}} = \frac{C^2 V k_3{}^3 N^2 L^2(\omega_3, \omega_2, \omega_1)}{288\pi^2 \hbar} \sin^2\theta |\varepsilon_{\lambda\mu\nu}\beta^{\mu\alpha}_{\lambda\mu\nu}|^2 \tag{16}$$

Here, it is noted that the experimentally measured property is the DFG susceptibility, not the molecular hyperpolarizability. When the chromophore concentration is sufficiently low so that it does not form any molecular aggregates, the DFG susceptibility is linearly proportional to the relevant molecular hyperpolarizability, as $\chi = NL(\omega_3,\omega_2,\omega_1)\langle\beta\rangle/\varepsilon_0$ where $L(\omega_3,\omega_2,\omega_1) = l(\omega_3)l(\omega_2)l(\omega_1)$ and $l(\omega)$ is the Lorentz local field correction factor. Thus, the LP DFG signal intensity is proportional to $L^2(\omega_3,\omega_2,\omega_1)$, and in eq 16 *N* is the molecular number density.

From eq 16, one can find that the LP DFG signal intensity does not vanish when $\varepsilon_{\lambda\mu\nu}\beta^{\mu\alpha}_{\lambda\mu\nu}$ is nonzero, where

$$\varepsilon_{\lambda\mu\nu}\beta^{\mu\alpha}_{\lambda\mu\nu} = \beta^{\mu\alpha}_{xyz} - \beta^{\mu\alpha}_{yxz} + \beta^{\mu\alpha}_{yzx} - \beta^{\mu\alpha}_{zyx} + \beta^{\mu\alpha}_{zxy} - \beta^{\mu\alpha}_{xzy} \tag{17}$$

From the definition of $\beta^{\mu\alpha}$ in eq 6, eq 17 can be rewritten as

$$\varepsilon_{\lambda\mu\nu}\beta^{\mu\alpha}_{\lambda\mu\nu} = \sum_{\mathrm{s}} \frac{1}{E_{\mathrm{s}0} - \hbar\omega_3 + i\Gamma_{\mathrm{s}}} \{\mu_x^{0\mathrm{s}}(\alpha_{yz}^{\mathrm{s}0} - \alpha_{zy}^{\mathrm{s}0}) + \mu_y^{0\mathrm{s}}(\alpha_{zx}^{\mathrm{s}0} - \alpha_{xz}^{\mathrm{s}0}) + \mu_z^{0\mathrm{s}}(\alpha_{xy}^{\mathrm{s}0} - \alpha_{yx}^{\mathrm{s}0})\} \tag{18}$$

Within the Born−Oppenheimer approximation, the electronically nonresonant Raman polarizability is a symmetric tensor so that eq 18 and the resultant LP DFG signal vanish. However, because of the breakdown of the BO approximation and nonzero antisymmetric Raman tensor elements, the LP DFG signal can be detectably large.[16,42,43] Nevertheless, this chiral component is approximately 3 orders of magnitude smaller than the symmetric Raman tensor elements. Consequently, the LP DFG field amplitude is likely to be very small by the same factor in comparison to the all-electric-dipole-allowed surface DFG field amplitude.[16] More specifically, Belkin et al. carried out IR-vis sum frequency generation (SFG) measurement of C−H stretch vibrations in limonene liquid and found that the antisymmetric polarizability tensor elements are $\sim 1 \times 10^{-53}$ $\mathrm{m^3C/V^2}$, whereas the achiral elements are $\sim 2 \times 10^{-50}$ $\mathrm{m^3C/V^2}$. Since the LP DFG field amplitude is also proportional to the antisymmetric

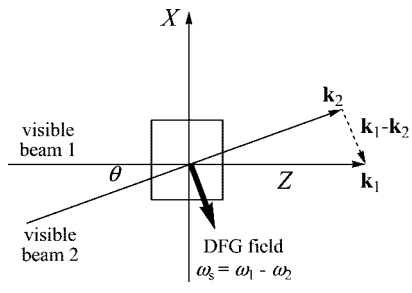

Figure 3. Perpendicular detection scheme for the VOA-DFG spectroscopy. The incident visible-1 radiation propagates along the laboratory *Z*-axis, and the angle between the visible-1 and -2 propagation directions is set to be θ. In the cases of the LP, CP-visible-1, and CP-visible-2 DFG measurements, the *Y*-component of the DFG field should be detected. On the other hand, the CP-field-detected DFG involves linearly polarized visible-1 and -2 radiations and the left or right CP component of the DFG field is selectively detected.

polarizability tensor elements, the measured LP DFG signal intensity is likely to be similar to the IR-vis SFG signal intensity reported in ref 16. Despite that the circularly polarized IR-vis SFG and the present LP-DFG are shown to be useful to study chiral molecules in an isotropic medium, strictly speaking they are not vibrational optical activity measurement methods. This is because, by definition, the optical activity is related to the difference in the response of a chiral molecule for orthogonal circular polarization states.

IV. DFG with Circularly Polarized Visible Radiations

Instead of using linearly polarized radiations, one can carry out a few different DFG measurements with circularly polarized ones. The second experimental scheme shown in Figure 1 corresponds to one of them, where the first radiation (visible-1) is polarization-modulated between LCP and RCP. The unit vectors of the LCP and RCP radiations are, respectively, given as

$$\mathbf{e}^{(1)}(L) = (\hat{X} + i\hat{Y})/\sqrt{2}$$
$$\mathbf{e}^{(1)}(R) = (\hat{X} - i\hat{Y})/\sqrt{2} \quad (19)$$

From the relationship between $\mathbf{b}$ and $\mathbf{e}$, (i.e., $\mathbf{b} = \hat{\mathbf{k}} \times \mathbf{e}$), we have $\mathbf{b}^{(1)}(L) = -i\hat{X}/\sqrt{2} + \hat{Y}/\sqrt{2}$ and $\mathbf{b}^{(1)}(R) = i\hat{X}/\sqrt{2} + \hat{Y}/\sqrt{2}$. Unlike the visible-1, the visible-2 radiation is assumed to be linearly polarized in this case (i.e., $\mathbf{e}^{(2)} = \hat{X}\cos\theta - \hat{Z}\sin\theta$). Except for this, the beam configuration and detection scheme is identical to that used for the LP DFG measurement discussed in the previous section. Then, for the LCP and RCP visible-1 measurements, the rotationally averaged DFG transition amplitudes are found to be

$$\langle M_{\mathrm{DFG}}(L/R)\rangle = -\frac{iC}{24}\sin\theta\varepsilon_{\lambda\mu\nu}\beta^{\mu\alpha}_{\lambda\mu\nu} \mp \frac{C}{24c}\sin\theta\varepsilon_{\lambda\mu\nu}\beta^{\mu G}_{\lambda\mu\nu} \mp \frac{C}{24c}(\hat{k}_{3X}\cos\theta + \hat{k}_{3Z}\sin\theta)\varepsilon_{\lambda\mu\nu}\beta^{m\alpha}_{\lambda\mu\nu} \pm \frac{ik_1C}{4}\sin\theta I^{(4)}_{YZYZ,\lambda\mu\nu\pi}\beta^{\mu A}_{\lambda\mu\nu\pi} \pm \frac{ik_2C}{4}\cos\theta\sin\theta\{I^{(4)}_{YXYX,\lambda\mu\nu\pi} - I^{(4)}_{YZYZ,\lambda\mu\nu\pi}\}\beta^{\mu\bar{A}}_{\lambda\mu\nu\pi} \mp \frac{ik_3C}{4}\{\hat{k}_{3Z}\sin\theta I^{(4)}_{YZZY,\lambda\mu\nu\pi} - \hat{k}_{3X}\cos\theta I^{(4)}_{YXXY,\lambda\mu\nu\pi}\}\beta^{Q\alpha}_{\lambda\mu\nu\pi} \quad (20)$$

On the right-hand side of eq 20, the upper (lower) signs correspond to the case where the incident visible-1 is LCP (RCP). We shall use this sign notation throughout this article. The unit vector of $\mathbf{k_3}$ was denoted as $\hat{k}_3$, and $\hat{k}_{3Z}$, and $\hat{k}_{3X}$, which are the Z and X components of $\hat{k}_3$, are given as

$$\hat{k}_{3X} = \frac{-k_2\sin\theta}{\sqrt{k_1^2 + k_2^2 - k_1k_2\cos\theta}}$$
$$\hat{k}_{3Z} = \frac{k_1 - k_2\cos\theta}{\sqrt{k_1^2 + k_2^2 - k_1k_2\cos\theta}} \quad (21)$$

For randomly oriented chiral molecules in an isotropic medium, the rotationally averaged fourth-rank tensor element $T^{(4)}_{ijkl}$ in a space-fixed frame is related to the corresponding fourth-rank tensor elements in a molecule-fixed frame as

$$T^{(4)}_{ijkl} = I^{(4)}_{ijkl,\lambda\mu\nu\pi}t^{(4)}_{\lambda\mu\nu\pi} \quad (22)$$

The indices i, j, k, and l represent one of the axes X, Y, and Z in a space-fixed frame, whereas λ, μ, ν, and π are the axes x, y, and z in a molecule-fixed frame. The connection term $I^{(4)}_{ijkl,\lambda\mu\nu\pi}$ in eq 22, which was obtained by considering rotational averages of direction cosines, is given as[39]

$$I^{(4)}_{ijkl,\lambda\mu\nu\pi} = \frac{1}{30}(\delta_{ij}\delta_{kl} \quad \delta_{ik}\delta_{jl} \quad \delta_{il}\delta_{jk})\begin{pmatrix} 4 & -1 & -1 \\ -1 & 4 & -1 \\ -1 & -1 & 4 \end{pmatrix}\begin{pmatrix} \delta_{\lambda\mu}\delta_{\nu\pi} \\ \delta_{\lambda\nu}\delta_{\mu\pi} \\ \delta_{\lambda\pi}\delta_{\mu\nu} \end{pmatrix} \quad (23)$$

Now, let us examine the result in eq 20 in more detail. In addition to the all-electric-dipole contribution $\beta^{\mu\alpha}_{\lambda\mu\nu}$, one should take into account five more transition pathways contributing to the DFG transition amplitude in the present case. However, only three of them are quantitatively large so that the remaining terms can be ignored, as shown below. First, let us consider the second term in eq 20. In the far-from-resonance limit, the magnetic dipole-ROA tensors G and $\bar{G}$ are known to be symmetric. However, since the Levi−Civita tensor is antisymmetric with respect to the exchange of any two indices, the second term in eq 20 vanishes. Second, let us consider $\varepsilon_{\lambda\mu\nu}\beta^{m\alpha}_{\lambda\mu\nu}$ in the third term of eq 20. Note that

$$\varepsilon_{\lambda\mu\nu}\beta^{m\alpha}_{\lambda\mu\nu} = (\beta^{m\alpha}_{xyz} - \beta^{m\alpha}_{yxz}) + (\beta^{m\alpha}_{yzx} - \beta^{m\alpha}_{zyx}) + (\beta^{m\alpha}_{zxy} - \beta^{m\alpha}_{xzy}) \quad (24)$$

Although, because of the breakdown of the BO approximation, the antisymmetric Raman tensor elements such as $\alpha_{xy} - \alpha_{yx}$ can be nonzero, these values of chiral molecules are typically very small. Furthermore, $\varepsilon_{\lambda\mu\nu}\beta^{m\alpha}_{\lambda\mu\nu}$ is linearly proportional to the magnetic dipole, which is another small factor. Thus, the third term including $\varepsilon_{\lambda\mu\nu}\beta^{m\alpha}_{\lambda\mu\nu}$ in eq 20 is likely to be 2 to 3 orders of magnitude smaller than the all-electric-dipole term in the same equation. Thus, it will be ignored hereafter. The fifth term in eq 20 has $\{I^{(4)}_{YXYX,\lambda\mu\nu\pi} - I^{(4)}_{YZYZ,\lambda\mu\nu\pi}\}\beta^{\mu\bar{A}}_{\lambda\mu\nu\pi}$. From the definition of $I^{(4)}_{ijkl,\lambda\mu\nu\pi}$ in eq 23, we have the following equality:

$$I^{(4)}_{YXYX,\lambda\mu\nu\pi}\beta^{\mu\bar{A}}_{\lambda\mu\nu\pi} = I^{(4)}_{YZYZ,\lambda\mu\nu\pi}\beta^{\mu\bar{A}}_{\lambda\mu\nu\pi} \quad (25)$$

which suggests that the fifth term vanishes.

Consequently, the transition amplitude of the DFG process when the incident visible-1 field is CP is simplified as

$$\langle M_{\mathrm{DFG}}(L/R)\rangle = -\frac{iC}{4}\left\{\frac{1}{6}\sin\theta\varepsilon_{\lambda\mu\nu}\beta^{\mu\alpha}_{\lambda\mu\nu} \mp k_1\sin\theta I^{(4)}_{YZYZ,\lambda\mu\nu\pi}\beta^{\mu A}_{\lambda\mu\nu\pi} \pm k_3P_{\lambda\mu\nu\pi}\beta^{Q\alpha}_{\lambda\mu\nu\pi}\right\} \quad (26)$$

where $P_{\lambda\mu\nu\pi}$ is defined as

$$P_{\lambda\mu\nu\pi} = \hat{k}_{3Z}\sin\theta I^{(4)}_{YZZY,\lambda\mu\nu\pi} - \hat{k}_{3X}\cos\theta I^{(4)}_{YXXY,\lambda\mu\nu\pi} = \frac{k_1\sin\theta}{\sqrt{k_1^2 + k_2^2 - k_1k_2\cos\theta}}I^{(4)}_{YZZY,\lambda\mu\nu\pi} \quad (27)$$

Therefore, the LCP- and RCP-visible-1 DFG signal intensities are

$$I(L/R) = \frac{C^2Vk_3^3N^2L^2}{64\pi^2\hbar}\left\{\frac{1}{36}\sin^2\theta|\varepsilon_{\lambda\mu\nu}\beta^{\mu\alpha}_{\lambda\mu\nu}|^2 + k_1^2\sin^2\theta|I^{(4)}_{YZYZ,\lambda\mu\nu\pi}\beta^{\mu A}_{\lambda\mu\nu\pi}|^2 + k_3^2|P_{\lambda\mu\nu\pi}\beta^{Q\alpha}_{\lambda\mu\nu\pi}|^2 \mp \frac{1}{3}k_1\sin^2\theta Re[\varepsilon_{\lambda\mu\nu}\beta^{\mu\alpha}_{\lambda\mu\nu}I^{(4)}_{YZYZ,\phi\chi\theta\rho}\bar{\beta}^{\mu A}_{\phi\chi\theta\rho}] \pm \frac{1}{3}k_3\sin\theta Re[\varepsilon_{\lambda\mu\nu}\beta^{\mu\alpha}_{\lambda\mu\nu}P_{\phi\chi\theta\rho}\bar{\beta}^{Q\alpha}_{\phi\chi\theta\rho}] - 2k_1k_3\sin\theta Re[I^{(4)}_{YZYZ,\lambda\mu\nu\pi}\beta^{\mu A}_{\lambda\mu\nu\pi}P_{\phi\chi\theta\rho}\bar{\beta}^{Q\alpha}_{\phi\chi\theta\rho}]\right\} \quad (28)$$

The first three terms are related to the transition probabilities

associated with the three transition amplitudes in eq 26. However, there are additional interference terms, which are the last three terms in eq 28.

From the conventional definition of the optical activity, which is the differential optical interactions of left and right circularly polarized radiations by chiral molecules, we shall consider the circular intensity difference (CID) defined as

$$\Delta I \equiv I(L) - I(R) \tag{29}$$

Here, it should be noted that the conventional definition of ROA is, however, $I_{\mathrm{ROA}} \equiv I_{\mathrm{Raman}}(R) - I_{\mathrm{Raman}}(L)$. In the case of the CP-visible-1 DFG, the CID is found to be

$$\Delta I = -\frac{C^2 V k_3{}^3 N^2 L^2}{96\pi^2\hbar}\Big\{k_1 \sin^2\theta Re[\varepsilon_{\lambda\mu\nu}\beta^{\mu\alpha}_{\lambda\mu\nu} I^{(4)}_{YZYZ,\phi\chi\theta\rho}\bar{\beta}^{\mu A}_{\phi\chi\theta\rho}] - k_3 \sin\theta Re\big[\varepsilon_{\lambda\mu\nu}\beta^{\mu\alpha}_{\lambda\mu\nu} P_{\phi\chi\theta\rho}\bar{\beta}^{Q\alpha}_{\phi\chi\theta\rho}\big]\Big\}$$
$$= -\frac{C^2 V k_3{}^3 N^2 L^2}{96\pi^2\hbar} k_1 \sin^2\theta Re \times \left[\varepsilon_{\lambda\mu\nu}\beta^{\mu\alpha}_{\lambda\mu\nu} I^{(4)}_{YZYZ,\phi\chi\theta\rho}\left\{\bar{\beta}^{\mu A}_{\phi\chi\theta\rho} - \frac{k_3}{\sqrt{k_1{}^2 + k_2{}^2 - k_1 k_2\cos\theta}}\bar{\beta}^{Q\alpha}_{\phi\chi\theta\rho}\right\}\right] \tag{30}$$

It is interesting to note that only the two interference terms contribute to the circular intensity difference signal for the CP-visible-1 DFG measurement. At $\theta = 90°$, since $k_3/\sqrt{k_1{}^2 + k_2{}^2} \approx 10^{-1} - 10^{-2}$, the second term in the curly bracket of eq 30 can be negligibly smaller than the first one.

Because of the nonzero antisymmetric Raman tensor elements, the all-electric-dipole term $\varepsilon_{\lambda\mu\nu}\beta^{\mu\alpha}_{\lambda\mu\nu}$ does not vanish for chiral molecules in solution. In addition, the rotational averages of the fourth-rank tensors, $I^{(4)}_{YZYZ,\phi\chi\theta\rho}\bar{\beta}^{\mu A}_{\phi\chi\theta\rho}$ and $I^{(4)}_{YZYZ,\phi\chi\theta\rho}\bar{\beta}^{Q\alpha}_{\phi\chi\theta\rho}$, which involve an electronic transition quadrupole moment and a vibrational transition quadrupole moment, respectively, can be nonzero. More specifically, the magnitudes of the A-tensor elements or electric quadrupole moments are typically $\sim 10^{-2}$ (fine structure constant) times as large as those of achiral polarizability tensor elements. Thus, two terms $I^{(4)}_{YZYZ,\phi\chi\theta\rho}\bar{\beta}^{\mu A}_{\phi\chi\theta\rho}$ and $I^{(4)}_{YZYZ,\phi\chi\theta\rho}\bar{\beta}^{Q\alpha}_{\phi\chi\theta\rho}$ are similar to the all-electric-dipole term $\varepsilon_{\lambda\mu\nu}\beta^{\mu\alpha}_{\lambda\mu\nu}$. Thus, the CID signal in eq 30 is quantitatively similar to the LP-DFG signal whose intensity is close to the IR-vis SFG signal from chiral liquid limonene reported in ref 16. As a result, the CID signal for the CP-visible-1 DFG can provide information on the chirality of a given molecular system in an isotropic medium.

V. DFG with Circularly Polarized Visible-2 Radiation

The third energy level diagram in Figure 1 is the case where the second incident visible-2 radiation is CP, whereas the visible-1 is linearly polarized. The experimental beam configuration and detection scheme is identical to the case of the LP DFG measurement. In this case, we have $\mathbf{e}^{(2)}(L) = \cos\theta\hat{X}/\sqrt{2} + i\hat{Y}/\sqrt{2} - \sin\theta\hat{Z}/\sqrt{2}$ and $\mathbf{b}^{(2)}(L) = -i\cos\theta\hat{X}/\sqrt{2} + \hat{Y}/\sqrt{2} + i\sin\theta\hat{Z}/\sqrt{2}$ By following the same procedure used to obtain eq 26, one can find that, for the LCP- and RCP-visible-2 DFG processes, the corresponding transition amplitudes are

$$\langle M_{\mathrm{DFG}}(L/R)\rangle = -\frac{iC}{24}\sin\theta\varepsilon_{\lambda\mu\nu}\beta^{\mu\alpha}_{\lambda\mu\nu} \pm \frac{C}{24c}\sin\theta\varepsilon_{\lambda\mu\nu}\beta^{\mu\bar{G}}_{\lambda\mu\nu} \mp \frac{C}{24c}\hat{k}_{3X}\varepsilon_{\lambda\mu\nu}\beta^{m\alpha}_{\lambda\mu\nu} \mp \frac{ik_2C}{4}\sin\theta I^{(4)}_{YYXX,\lambda\mu\nu\pi}\beta^{\mu\bar{A}}_{\lambda\mu\nu\pi} \mp \frac{ik_3C}{4}\hat{k}_{3X}I^{(4)}_{YXYX,\lambda\mu\nu\pi}\beta^{Q\alpha}_{\lambda\mu\nu\pi} \tag{31}$$

The second term in eq 31 vanishes because of the symmetric or antisymmetric properties of G, $\bar{G}$, and Levi−Civita ε. The third term is negligibly small in comparison to the first term. Thus, eq 31 is approximately given as

$$\langle M_{\mathrm{DFG}}(L/R)\rangle = -\frac{iC}{4}\Big\{\frac{1}{6}\sin\theta\varepsilon_{\lambda\mu\nu}\beta^{\mu\alpha}_{\lambda\mu\nu} \pm k_2\sin\theta I^{(4)}_{YYXX,\lambda\mu\nu\pi}\beta^{\mu\bar{A}}_{\lambda\mu\nu\pi} \pm k_3\hat{k}_{3X}I^{(4)}_{YXYX,\lambda\mu\nu\pi}\beta^{Q\alpha}_{\lambda\mu\nu\pi}\Big\} \tag{32}$$

From this transition amplitude, we find that the circular intensity difference signal for the present case is

$$\Delta I = \frac{C^2 V k_3{}^3 N^2 L^2}{96\pi^2\hbar}\Big\{k_2\sin^2\theta Re\big[\varepsilon_{\lambda\mu\nu}\beta^{\mu\alpha}_{\lambda\mu\nu} I^{(4)}_{YYXX,\phi\chi\theta\rho}\bar{\beta}^{\mu\bar{A}}_{\phi\chi\theta\rho}\big] + k_3\hat{k}_{3X}\sin\theta Re\big[\varepsilon_{\lambda\mu\nu}\beta^{\mu\alpha}_{\lambda\mu\nu} I^{(4)}_{YYXX,\phi\chi\theta\rho}\bar{\beta}^{Q\alpha}_{\phi\chi\theta\rho}\big]\Big\}$$
$$= \frac{C^2 V k_3{}^3 N^2 L^2}{96\pi^2\hbar} k_2\sin^2\theta \times Re\left[\varepsilon_{\lambda\mu\nu}\beta^{\mu\alpha}_{\lambda\mu\nu} I^{(4)}_{YYXX,\phi\chi\theta\rho}\left\{\bar{\beta}^{\mu\bar{A}}_{\phi\chi\theta\rho} - \frac{k_3}{\sqrt{k_1{}^2 + k_2{}^2 - k_1 k_2\cos\theta}}\bar{\beta}^{Q\alpha}_{\phi\chi\theta\rho}\right\}\right] \tag{33}$$

This result is slightly different from that of the CP-visible-1 DFG, which is given in eq 30. Other than a few constant factors, the CP-visible-2 DFG is related to the electric quadrupole-ROA tensor $\bar{A}$, whereas eq 30 is related to A.

VI. Circularly Polarized Field-Detected DFG

Instead of using CP radiations to carry out VOA-DFG measurements, one can in principle detect the LCP and RCP components of the radiated DFG signal field, even though the two incident radiations are linearly polarized. Then, the unit vectors of the electric and magnetic field vectors, $\mathbf{e}^{(3)}(L)$ and $\mathbf{b}^{(3)}(L)$, when the LCP component of the radiated DFG signal electromagnetic field is detected, are $\mathbf{e}^{(3)}(L) = -i\hat{k}_{3Z}\hat{X}/\sqrt{2} + \hat{Y}/\sqrt{2} + i\hat{k}_{3X}\hat{Z}/\sqrt{2}$ and $\mathbf{b}^{(3)}(L) = -\hat{k}_{3Z}\hat{X}/\sqrt{2} - i\hat{Y}/\sqrt{2} + \hat{k}_{3X}\hat{Z}/\sqrt{2}$, respectively. This is the last case shown in Figure 1. The CP-field-detected DFG transition amplitudes are, then, found to be

$$\langle M_{\mathrm{DFG}}(L/R)\rangle = -\frac{iC}{24}\sin\theta\varepsilon_{\lambda\mu\nu}\beta^{\mu\alpha}_{\lambda\mu\nu} \pm \frac{C}{24c}(\hat{k}_{3X}\cos\theta - \hat{k}_{3Z}\sin\theta)\varepsilon_{\lambda\mu\nu}\beta^{\mu G}_{\lambda\mu\nu} \mp \frac{C}{24c}\hat{k}_{3X}\varepsilon_{\lambda\mu\nu}\beta^{\mu\bar{G}}_{\lambda\mu\nu} \mp \frac{C}{24c}\sin\theta\varepsilon_{\lambda\mu\nu}\beta^{m\alpha}_{\lambda\mu\nu} \pm \frac{ik_1C}{4}Q_{\lambda\mu\nu\pi}\beta^{\mu A}_{\lambda\mu\nu\pi} \pm \frac{ik_2C}{4}R_{\lambda\mu\nu\pi}\beta^{\mu\bar{A}}_{\lambda\mu\nu\pi} \pm \frac{ik_3C}{4}S_{\lambda\mu\nu\pi}\beta^{Q\alpha}_{\lambda\mu\nu\pi} \tag{34}$$

Here, the auxiliary functions resulting from the rotational averaging calculations are defined as

$$Q_{\lambda\mu\nu\pi} = \hat{k}_{3Z}\sin\theta I^{(4)}_{XZXZ,\lambda\mu\nu\pi} + \hat{k}_{3X}\cos\theta I^{(4)}_{ZXXZ,\lambda\mu\nu\pi} \tag{35}$$

$$R_{\lambda\mu\nu\pi} = \hat{k}_{3Z}\cos\theta\sin\theta I^{(4)}_{XXXX,\lambda\mu\nu\pi} + \hat{k}_{3X}\sin^2\theta I^{(4)}_{ZZXX,\lambda\mu\nu\pi} - \hat{k}_{3X}\cos^2\theta I^{(4)}_{ZXXZ,\lambda\mu\nu\pi} - \hat{k}_{3Z}\cos\theta\sin\theta I^{(4)}_{XZXZ,\lambda\mu\nu\pi} \tag{36}$$

$$S_{\lambda\mu\nu\pi} = \hat{k}_{3X}\hat{k}_{3Z}\cos\theta I^{(4)}_{XXXX,\lambda\mu\nu\pi} + \hat{k}^2_{3X}\sin\theta I^{(4)}_{ZXZX,\lambda\mu\nu\pi} - \hat{k}_{3X}\hat{k}_{3Z}\cos\theta I^{(4)}_{ZZXX,\lambda\mu\nu\pi} - \hat{k}^2_{3Z}\sin\theta I^{(4)}_{XZZX,\lambda\mu\nu\pi} \quad (37)$$

Invoking the same approximations mentioned in section IV, one can find that the transition amplitude is determined by four dominant terms:

$$\langle M_{\mathrm{DFG}}(L/R)\rangle = -\frac{iC}{4}\left\{\frac{1}{6}\sin\theta\varepsilon_{\lambda\mu\nu}\beta^{\mu\alpha}_{\lambda\mu\nu} \mp k_1 Q_{\lambda\mu\nu\pi}\beta^{\mu A}_{\lambda\mu\nu\pi} \mp k_2 R_{\lambda\mu\nu\pi}\beta^{\mu\bar{A}}_{\lambda\mu\nu\pi} \mp k_3 S_{\lambda\mu\nu\pi}\beta^{Q\alpha}_{\lambda\mu\nu\pi}\right\} \quad (38)$$

From the transition amplitudes given above, the corresponding homodyne-detected DFG signals can be obtained as

$$\begin{aligned} I(L/R) = \frac{C^2 V k_3{}^3 N^2 L^2}{64\pi^2\hbar}\Big\{&\frac{1}{36}\sin^2\theta|\varepsilon_{\lambda\mu\nu}\beta^{\mu\alpha}_{\lambda\mu\nu}|^2 + k_1{}^2|Q_{\lambda\mu\nu\pi}\beta^{\mu A}_{\lambda\mu\nu\pi}|^2 + k_2{}^2|R_{\lambda\mu\nu\pi}\beta^{\mu\bar{A}}_{\lambda\mu\nu\pi}|^2 \\ &+ k_3{}^2|S_{\lambda\mu\nu\pi}\beta^{Q\alpha}_{\lambda\mu\nu\pi}|^2 \mp \frac{1}{3}k_1\sin\theta Re[\varepsilon_{\lambda\mu\nu}\beta^{\mu\alpha}_{\lambda\mu\nu}Q_{\phi\chi\theta\rho}\bar{\beta}^{\mu A}_{\phi\chi\theta\rho}] \mp \\ &\frac{1}{3}k_2\sin\theta Re[\varepsilon_{\lambda\mu\nu}\beta^{\mu\alpha}_{\lambda\mu\nu}R_{\phi\chi\theta\rho}\bar{\beta}^{\mu\bar{A}}_{\phi\chi\theta\rho}] \mp \\ &\frac{1}{3}k_3\sin\theta Re[\varepsilon_{\lambda\mu\nu}\beta^{\mu\alpha}_{\lambda\mu\nu}S_{\phi\chi\theta\rho}\bar{\beta}^{Q\alpha}_{\phi\chi\theta\rho}] + \\ &2k_1k_2 Re[Q_{\lambda\mu\nu\pi}\beta^{\mu A}_{\lambda\mu\nu\pi}R_{\phi\chi\theta\rho}\bar{\beta}^{\mu\bar{A}}_{\phi\chi\theta\rho}] + \\ &2k_1k_3 Re[Q_{\lambda\mu\nu\pi}\beta^{\mu A}_{\lambda\mu\nu\pi}S_{\phi\chi\theta\rho}\bar{\beta}^{Q\alpha}_{\phi\chi\theta\rho}] + \\ &2k_2k_3 Re[R_{\lambda\mu\nu\pi}\beta^{\mu\bar{A}}_{\lambda\mu\nu\pi}S_{\phi\chi\theta\rho}\bar{\beta}^{Q\alpha}_{\phi\chi\theta\rho}]\Big\} \quad (39) \end{aligned}$$

The circular intensity difference signal is, thus, given as

$$\Delta I = -\frac{C^2 V k_3{}^3 N^2 L^2}{96\pi^2\hbar}\sin\theta\{k_1 Re[\varepsilon_{\lambda\mu\nu}\beta^{\mu\alpha}_{\lambda\mu\nu}Q_{\phi\chi\theta\rho}\bar{\beta}^{\mu A}_{\phi\chi\theta\rho}] + k_2 Re[\varepsilon_{\lambda\mu\nu}\beta^{\mu\alpha}_{\lambda\mu\nu}R_{\phi\chi\theta\rho}\bar{\beta}^{\mu\bar{A}}_{\phi\chi\theta\rho}] + k_3 Re[\varepsilon_{\lambda\mu\nu}\beta^{\mu\alpha}_{\lambda\mu\nu}S_{\phi\chi\theta\rho}\bar{\beta}^{Q\alpha}_{\phi\chi\theta\rho}]\} \quad (40)$$

The nonlinear optical activity that can be extracted from the CP-field-detected DFG is determined by three interference terms. The DFG electric field generated by the nonzero chiral all-electric-dipole hyperpolarizability $\varepsilon_{\lambda\mu\nu}\beta^{\mu\alpha}_{\lambda\mu\nu}$ interferes with the three fields produced by other hyperpolarizabilities involving one electric quadrupole transition.

As discussed in this and previous sections, we considered three different VOA-DFG schemes that are different from one another by the polarization state of the three radiations involved in a DFG process. Only one of the three radiations is circularly polarized. However, it could be possible to consider other possibilities where all three radiations are either left or right circularly polarized. In relation to these possibilities, it is noted that there are four forms of ROA and they are incident circular polarization ROA, scattered circular polarization ROA, and in-phase and out-of-phase dual circular polarization ROAs (see ref 4). The latter two cases correspond to the ROA measurements when both of the incident and scattered radiations are circularly polarized. Similarly, in the present case of circularly polarized DFG schemes, it will be possible to measure the all-LCP or all-RCP ROA signals where not only the two incident visible radiations but also the generated DFG field are circularly polarized. These types of VOA-DFG methods are currently under investigation.

SCHEME 1

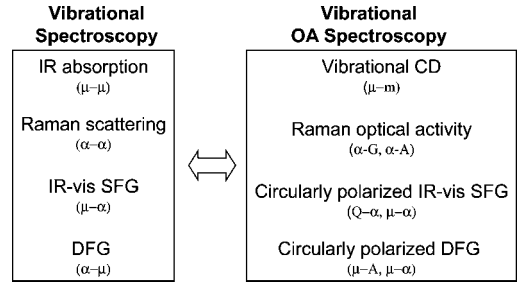

VII. Concluding Remarks and Summary

In the present article, we considered the VOA-DFG spectroscopy for chiral molecules in solutions theoretically. Depending on the polarization states of the incident and detected signal fields, one can measure the DFG susceptibility originating from the chiral all-electric-dipole hyperpolarizability or from interferences between that and other hyperpolarizabilities involving an electric quadrupole transition. Since the DFG signal can be resonantly enhanced when the difference frequency is close to one of the vibrational frequencies of a given chiral molecule in solution, the present DFG measurement technique can be considered as a *vibrational* optical activity measurement tool.

In Scheme 1, the one-to-one correspondence relationships between the conventional vibrational spectroscopic methods and the vibrational optical activity measurement methods are shown. In the cases of the IR absorption and Raman scattering, the spectra are related to the dipole−dipole and polarizability−polarizability time-correlation functions (TCF) via Fourier transformations. The IR-vis SFG susceptibility is related to the Fourier transform of dipole-polarizability TCF. Similarly, the vibrationally resonant DFG susceptibility can also be described in terms of the polarizability-dipole TCF. These four different vibrational spectroscopic methods in the left box of Scheme 1 are, however, not sensitive to molecular chirality or handedness. On the other hand, those on the right-hand side of Scheme 1 are optical activity measurement techniques. The VCD is related to the cross TCF of electric dipole and magnetic dipole moments. The ROA is determined by the cross TCFs of polarizability and various ROA tensors. The circularly polarized IR-vis SFGs discussed in refs 34 and 35 were found to be determined by both chiral component of the dipole-polarizability TCF as well as polarizability-electric quadrupole TCF. In the present work, we showed that, in addition to the VOA measurements such as VCD, ROA, and CP IV-SFG, the circularly polarized VOA-DFG can be a useful and complementary tool for studies of nonlinear optical activity of chiral molecules in solutions.

Acknowledgment. This work was supported by the Creative Research Initiatives Program of KISTEP (MOST, Korea).

References and Notes

(1) *Circular Dichroism: Principles and Applications*; Berova, N., Nakanishi, K., Woody, R. W., Eds.; Wiley-VCH: New York, 2000.
(2) Rosenfeld, L. *Z. Phys.* **1928**, *52*, 161.
(3) Mantsch, H. H.; Chapman, D. *Infrared Spectroscopy of Biomolecules*; Wiley-Liss: New York, 1996.
(4) Nafie, L. A. *Annu. Rev. Phys. Chem.* **1997**, *48*, 357.
(5) Keiderling, T. A. *Curr. Opin. Chem. Biol.* **2002**, *6*, 682.
(6) Eker, F.; Griebenow, K.; Cao, X. L.; Nafie, L. A.; Schweitzer-Stenner, R. *Proc. Natl. Acad. Sci. U.S.A.* **2004**, *101*, 10054.
(7) Kubelka, J.; Keiderling, T. A. *Biophys. J.* **2002**, *82*, 179A.
(8) Choi, J. H.; Hahn, S.; Cho, M. *Int. J. Quantum Chem.* **2005**, *104*, 616.

(9) Schweitzer-Stenner, R. *Vib. Spectrosc.* **2006**, *42*, 98.
(10) Barron, L. D.; Bogaard, M. P.; Buckingham, A. D. *J. Am. Chem. Soc.* **1973**, *95*, 603.
(11) Barron, L. D.; Hecht, L.; Blanch, E. W.; Bell, A. F. *Prog. Biophys. Mol. Biol.* **2000**, *73*, 1.
(12) McColl, I. H.; Blanch, E. W.; Hecht, L.; Kallenbach, N. R.; Barron, L. D. *J. Am. Chem. Soc.* **2004**, *126*, 5076.
(13) Zhu, F.; Isaacs, N. W.; Hecht, L.; Barron, L. D. *J. Am. Chem. Soc.* **2005**, *127*, 6142.
(14) Barron, L. D.; Hecht, L. Vibrational Raman Optical Activity: From Fundamentals to Biochemical Applications. In *Circular Dichroism: Principles and Applications*; Berova, N., Nakanishi, K., Woody, R. W., Eds.; Wiley-VCH: New York, 2000; p 667.
(15) Nafie, L. A.; Freedman, T. B. Vibrational Optical Activity Theory. In *Circular Dichroism: Principles and Applications*; Berova, N., Nakanishi, K., Woody, R. W., Eds.; Wiley-VCH: New York, 2000; p 97.
(16) Belkin, M. A.; Kulakov, T. A.; Ernst, K.-H.; Yan, L.; Shen, Y. R. *Phys. Rev. Lett.* **2000**, *85*, 4474.
(17) Belkin, M. A.; Han, S. H.; Wei, X.; Shen, Y. R. *Phys. Rev. Lett.* **2001**, *87*, 113001.
(18) Belkin, M. A.; Shen, Y. R. *Phys. Rev. Lett.* **2003**, *91*, 213907.
(19) Fischer, P.; Hache, F. *Chirality* **2005**, *17*, 421.
(20) Ji, N.; Shen, Y. R. *J. Am. Chem. Soc.* **2004**, *126*, 15008.
(21) Wang, J.; Chen, X.; Clarke, M. L.; Chen, Z. *Proc. Natl. Acad. Sci. U.S.A.* **2005**, *102*, 4978.
(22) Superfine, R.; Guyotsionnest, P.; Hunt, J. H.; Kao, C. T.; Shen, Y. R. *Surf. Sci.* **1988**, *200*, L445.
(23) Shen, Y. R. *Nature* **1989**, *337*, 519.
(24) Zhu, X. D.; Suhr, H.; Shen, Y. R. *Phys. Rev. B* **1987**, *35*, 3047.
(25) Backus, E. H. G.; Eichler, A.; Kleyn, A. W.; Bonn, M. *Science* **2005**, *310*, 1790.
(26) Miragliotta, J.; Polizzotti, R. S.; Rabinowitz, P.; Cameron, S. D.; Hall, R. B. *Chem. Phys.* **1990**, *143*, 123.
(27) Koffas, T. S.; Kim, J.; Lawrence, C. C.; Somorjai, G. A. *Langmuir* **2003**, *19*, 3563.
(28) Dreesen, L.; Humbert, C.; Hollander, P.; Mani, A. A.; Ataka, K.; Thiry, P. A.; Peremans, A. *Chem. Phys. Lett.* **2001**, *333*, 327.
(29) Yang, M. C.; Tang, D. C.; Somorjai, G. A. *Rev. Sci. Instrum.* **2003**, *74*, 4554.
(30) Morita, A.; Ishiyama, T. *Phys. Chem. Chem. Phys.* **2008**, *10*, 5801.
(31) Gracias, D. H.; Chen, Z.; Shen, Y. R.; Somorjai, G. A. *Acc. Chem. Res.* **1999**, *32*, 930.
(32) Wang, J.; Paszti, Z.; Even, M. A.; Chen, Z. *J. Am. Chem. Soc.* **2002**, *124*, 7016.
(33) Chen, Z.; Shen, Y. R.; Somorjai, G. A. *Annu. Rev. Phys. Chem.* **2002**, *53*, 437.
(34) Cho, M. *J. Chem. Phys.* **2002**, *116*, 1562.
(35) Cheon, S.; Cho, M. *Phys. Rev. A* **2005**, *71*, 013808.
(36) Cheon, S.; Lee, H.; Choi, J. H.; Cho, M. *J. Chem. Phys.* **2007**, *126*, 054505.
(37) Cho, M. *Chem. Rev.* **2008**, *108*, 1331.
(38) Loudon, R. *The Quantum Theory of Light*; Clarendon Press: Oxford, 1983.
(39) Craig, D. P.; Thirunamachandran, T. *Molecular Quantum Electrodynamics: An Introduction to Radiation Molecule Interactions*; Dover Publications: New York, 1998.
(40) Shen, Y. R. *The Principles of Nonlinear Optics*; Wiley & Sons: New York, 1984.
(41) Nafie, L. A. *Theor. Chem. Acc.* **2008**, *119*, 39.
(42) Liu, F.-C. *J. Phys. Chem.* **1991**, *95*, 7180.
(43) Liu, F.-C.; Buckingham, A. D. *Chem. Phys. Lett.* **1993**, *207*, 325.

JP809652X